nature communications

Article

https://doi.org/10.1038/s41467-025-64742-y

Amygdala AVPR1A mediates susceptibility to chronic social isolation in female mice

Received: 15 August 2025

Accepted: 23 September 2025

Published online: 04 November 2025

Check for updates

Marie François[1], Kelly L. Vranich[1,10], Isabella Canal Delgado[1,10], Alexandre Lafond[1,10], Natalie R. Lopatinsky[1,10], Tronjay Davis[1], Eastman M. Lewis[2,3], Mia Kuromaru[1], Rim Hassouna[1], Brenna Williams[4], Sebastian E. Ho[1], Lucas A. C. Souza[1], Daniele Neri[1], Youjin Oh[5], Christopher D. Makinson[5], Kevin G. Bath[6,7], Gül Dölen[8] & Lori M. Zeltser[1,9]

Sex differences in responsiveness to social stress in adulthood are highly conserved across species, with females more sensitive to isolation. Here, we show that Arginine vasopressin receptor 1a (AVPR1A) in the central nucleus of the amygdala (CeA) mediates the enhanced susceptibility of females to post-pubertal chronic social isolation stress (CSIS) in mice. Chemogenetic activation of AVPR1A^{CeA} circuits induces anxiety-related behaviors in both sexes. However, genetic, pharmacological, chemogenetic and optogenetic loss of function approaches support the idea that it is only endogenously engaged in females in the context of CSIS. Using a combination of virus-based tools, we identified a major source of AVP ligand in the posterodorsal part of the medial amygdala (MePD) as well as an important downstream target of AVPR1A^{CeA} neurons, the dorsolateral striatum (DLS). Loss of function approaches identified three nodes in the circuit that provide sex-specificity in the effects of CSIS on anxiety-related behaviors: 1) ERα signaling in AVP^{MePD} neurons; 2) engagement of the AVPR1A pathway in the CeA; and 3) number of AVPR1A^{CeA} projections to the DLS. These data support new therapeutic applications for AVPR1A antagonists in women experiencing social isolation or loneliness.

Sex differences in responsiveness to social stressors are well-documented. For example, men react more to achievement or ego-threatening stress, while women respond more to social exclusion stress[1–3]. Consistent with this, mental health in women was disproportionately impacted by the social restrictions imposed to control COVID-19 outbreaks[4]. Sex-specific responses to social isolation stress have also been observed in pre-clinical rodent models[5–7] and are thought to reflect differences in brain circuits regulating and responding to changing social relationships across development. During the juvenile period (P21-35), pups engage in playful interactions with cage mates that are critical to the maturation of social behaviors[8]. Social isolation during this period disrupts the establishment of these

[1]Naomi Berrie Diabetes Center, Columbia University Irving Medical Center, New York, NY, USA. [2]The Eunice K. Shriver National Institute for Child Health and Human Development, The National Institutes of Health, Bethesda, MD, USA. [3]The Solomon H. Snyder Department of Neuroscience, Johns Hopkins University School of Medicine, Baltimore, MD, USA. [4]Department of Cellular and Molecular Physiology and Biophysics, Columbia University Irving Medical Center, New York, NY, USA. [5]Departments of Neurology and Neuroscience, Columbia University Irving Medical Center, New York, NY, USA. [6]Department of Psychiatry, Columbia University Irving Medical Center, New York, NY, USA. [7]Division of Developmental Neuroscience, Department of Psychiatry, New York State Psychiatric Institute, New York, NY, USA. [8]Departments of Neuroscience, Department of Psychology, Berkeley Center for the Science of Psychedelics (BCSP), Helen Wills Neuroscience Institute (HWNI), University of California Berkeley, Berkeley, CA, USA. [9]Department of Pathology and Cell Biology, Columbia University Irving Medical Center, New York, NY, USA. [10]These authors contributed equally: Kelly L. Vranich, Isabella Canal Delgado, Alexandre Lafond, Natalie R. Lopatinsky. e-mail: lz146@cumc.columbia.edu

behaviors, with lasting effects on behavioral responses to stress[9]. Males establish territorial and dominant-subordinate relationships during the pubertal transition[10], so subsequent elimination of these interactions does not promote anxiety-related behavioral adaptations[11]. In contrast, females maintain positive social relationships with siblings into adulthood, and groups of females typically live together in communal nests[12]. Social isolation after puberty deprives female rodents of these relationships, and thus induces behavioral disturbances that are thought to model anxiety[13]. We previously demonstrated that stress-induced suppression of feeding, a common proxy for anxiety-related behavior, is exacerbated in females, but not males, exposed to long (>7 weeks) periods of social isolation[14].

Here, we set out to identify neural circuits that could mediate increased susceptibility of post-pubertal females to chronic social isolation stress (CSIS). We focused on the arginine vasopressin receptor 1 A (AVPR1A) system and the amygdala, because they have been implicated in sex differences in responsiveness to social stressors[15–17]. We found that stimulating AVPR1A^{CeA} neural circuits was sufficient to induce anxiety-related behaviors in group-housed males and females, but targeted loss of *Avpr1a* in the CeA reversed the anxiogenic effects of CSIS in females but had no effect in males. Using a combination of molecular, neuroanatomical, optogenetic, and intersectional gene knockdown approaches, we identified molecular, circuit, and hormonal mechanisms underlying sexually dimorphic responses to chronic social isolation.

Results

AVPR1A^{CeA} neurons elicit anxiety in both sexes

Intra-CeA AVP injections in male rats act in an AVPR1A-dependent manner to increase anxiety-related behavior in the elevated plus maze (EPM)[18]. We performed pilot studies to explore whether AVP → AVPR1A signals in the CeA have similar effects in females. Since behavior in females is often variable, we utilized the marble burying test, where repeated measurements can increase statistical power. Injections of AVP into the CeA increased marble burying compared to saline treatment in wildtype (WT) females but not *Avpr1a*−/− global mutants (Supplementary Fig. 1a–d). With this positive result in hand, we generated an *Avpr1a*-Cre mouse strain to provide genetic access to this subpopulation. We validated this line with single molecule fluorescent in situ hybridization (smFISH) using *Cre* and *Avpr1a* RNAscope probes and confirmed that over 90% of *Avpr1a*-expressing cells co-express Cre, with little (<10%) expression in non-*Avpra1*+ neurons (Supplementary Fig. 1e, f). We crossed the *Avpr1a*-Cre strain to a Cre-dependent tdTomato reporter line (*Avpr1a-Cre*::tdTOM) and mapped the distribution of tdTomato-expressing neurons across the amygdala in males and females. Neurons with the *Avpr1a* lineage trace were almost exclusively detected in the CeA, with a peak between bregma −1.46 and −1.58, with no significant sex differences (Fig. 1a, b), consistent with radiolabeled ligand binding studies in rats[19] and humans[20].

We next asked whether chemogenetic activation of AVPR1A^{CeA} neurons was sufficient to elicit anxiety-related behaviors in both sexes. We focused on the elevated plus maze (EPM) and marble burying tests, respectively, where meta-analyses support their external validity to screen for anxiolytic effects[21,22]. We performed bilateral intra-CeA injections of an AAV virus expressing a Cre-dependent Designer Receptors Exclusively Activated by Designer Drugs (DREADD)-Gq receptor or a control virus in group-housed *Avpr1a*-Cre mice (Fig. 1c–e and Supplementary Fig. 1g). A single injection of the DREADD ligand, clozapine-N-oxide (CNO, 1.5 mg/kg, i.p.), acutely activated AVPR1A^{CeA} neurons in mice injected with the DREADD-Gq virus but not the control virus (Supplementary Fig. 1i, j). The number of infected neurons was similar between males and females (Supplementary Fig. 1h). Chemogenetic activation of AVPR1A^{CeA} neurons increased marble burying and decreased time spent in the open arms of the EPM (Fig. 1f, g).

CSIS increases *Avpr1a* in the female CeA

Chronic social isolation imposed in the post-weaning period increases *Avpr1a* expression in males and not females[23]. Since females are preferentially affected when the onset of chronic social isolation is delayed to the post-pubertal period[11], we asked whether this is also reflected in *Avpr1a* expression in CeA micropunches (Fig. 2a, b). Expression levels were similar in group housed males and females but were increased by CSIS in females in a sex-dependent manner (Fig. 2c). Elevated *Avpr1a* levels persisted even after mice were re-grouped for 3 weeks (Fig. 2d). In contrast, exposure to social crowding from 5 weeks to 12 weeks or repeated restraint for 5 days at 11 weeks of age did not affect *Avpr1a* expression in either sex (Supplementary Fig. 2).

We explored whether the time of onset or duration of stress influences *Avpr1a* expression in the female CeA, since it can influence the nature of behavioral responses[8,24–26]. Exposure to 7 weeks of social isolation also increased *Avpr1a* expression when the onset of the stress was delayed from post-puberty (5 weeks) to young adulthood (8 weeks) (Fig. 2e). However, when the duration of adult social isolation was shortened to 2 weeks (10 weeks to 12 weeks), the effect on *Avpr1a* expression was no longer significant (Fig. 2e). Therefore, when social isolation is imposed after puberty, the length of the exposure is important, while the onset is not.

Since stimulation of AVPR1A^{CeA} circuits was sufficient to alter behavior in the EPM and marble burying assays (Fig. 1), we explored whether increased *Avpr1a* expression in females exposed to post-pubertal CSIS is associated with sex-specific effects on these behaviors (Fig. 2f). CSIS significantly increased marble burying in females and not males; while there was a trend toward interactions between CSIS and sex, it did not reach significance (Fig. 2g). At baseline, males spent less time in the open arms of the EPM than females. CSIS increased anxiety-related behavior in the EPM in females in a sex-dependent manner (Fig. 2h). In a separate cohort of mice, we tested whether anxiety-related behavioral adaptations in CSIS females could be reversed by housing them in groups of 3 for 3 weeks (Fig. 2i). To this end, we performed a marble burying test at the end of the CSIS (12 weeks of age) and then assigned half to remain in the socially isolated condition, while the remainder were switched to group housing. Three weeks later, both groups were re-tested at 15 weeks of age. The number of marbles buried was increased in both groups over time but was not reduced by re-grouping (Fig. 2j), showing the persistence of the effects of CSIS.

We then explored whether CSIS produces sex-specific effects on other common neurobehavioral tests (Supplementary Fig. 3a). Sucrose preference was decreased by CSIS (Supplementary Fig. 3b), but this behavior was not influenced by sex. In the open field test (OFT), we observed effects of stress and sex on time spent in the center, but no interaction between them (Supplementary Fig. 3c). Novelty-induced locomotor behavior increased similarly in CSIS males and females (Supplementary Fig. 3d). Behavioral performance in the novel object, rotarod, and forced swim tests were not influenced by sex or housing status (Supplementary Fig. 3e–g).

AVPR1A mediates effects of CSIS on females

We used a combination of genetic and pharmacological approaches to test the hypothesis that AVPR1A in the CeA mediates the sex-specific effects of CSIS on behaviors in the EPM and marble burying assays. While interactions between stress and sex only reached significance in the EPM, we included the marble burying assay because it provides more flexibility due to the ability to perform repeated testing. We generated a mouse line to conditionally delete *Avpr1a* (*Avpr1a^{Flox}*). To validate this model, we performed bilateral injections of AAV-Cre-GFP vs. control AAV-GFP into the CeA of *Avpr1a$^{Flox/Flox}$* homozygotes (Fig. 3a, b). The number of infected neurons was similar between control and Cre groups, and between males and females (Fig. 3c). *Avpr1a* expression was reduced by an average of 75% (Fig. 3d). Loss of both copies of

https://doi.org/10.1038/s41467-025-64742-y

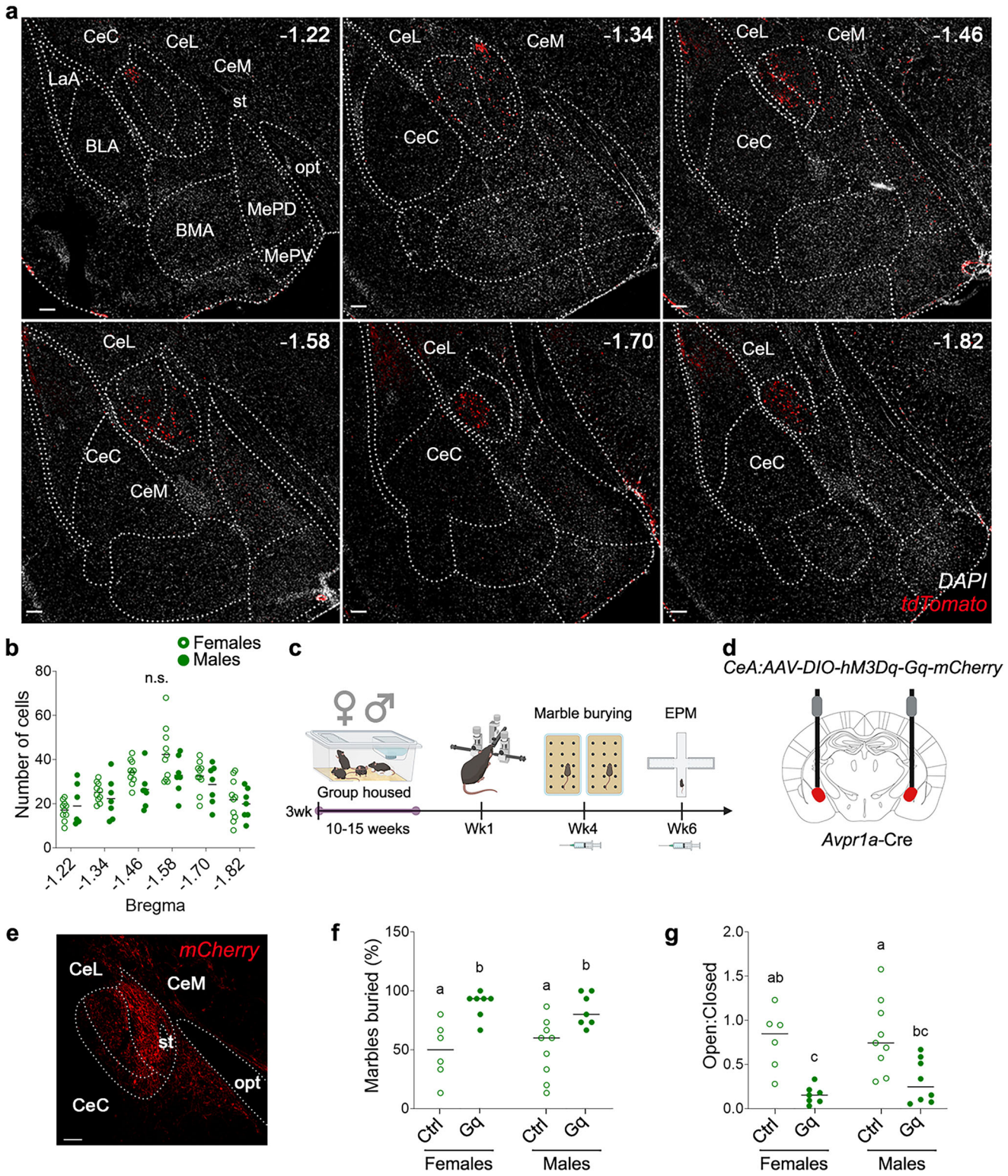

Fig. 1 | Stimulating AVPR1A^{CeA} neurons promotes anxiety-related behaviors in both sexes. a Neurons expressing the *Avpr1a*-Cre::tdTomato lineage trace are localized to the CeA in coronal sections of the amygdala from bregma −1.22 to −1.82. **b** No sex difference in *Avpr1a*-Cre::tdTomato lineage traced neurons in the amygdala ($P = 0.3802$, $n = 7$ males, n = 10 females). **c** Experimental design to assess the effect of chemogenetic activation of AVPR1A^{CeA} neurons in group-housed mice on anxiety-related behaviors. **d** Schematic of viral injection into the CeA of *Avpr1a*-Cre mice. **e** Representative expression of the viral mCherry reporter in the CeA ($n = 26$). **f**, **g** Chemogenetic activation of AVPR1A^{CeA} neurons increased marble burying (**f**) and reduced time spent in the open arms of the EPM (**g**) (marble burying: group $P = < 0.0001$, sex $P = 0.8657$, interaction group*sex $P = 0.6425$; EPM: group $P = < 0.0001$, sex $P = 0.3904$, interaction group*sex $P = 0.6247$, $n = 6$ control females, $n = 7$ Gq females, $n = 9$ control males, $n = 8$ Gq males). An unpaired two-tailed t-test was used in (**b**). Two-way ANOVA (with RM for marble burying) and Tukey's multiple comparisons were used in (**f**, **g**). Different letters denote significant differences. n denotes the number of mice in each group. Scale bars represent 100 µm. Schematic in (**c**) was generated with BioRender icons[49].

https://doi.org/10.1038/s41467-025-64742-y

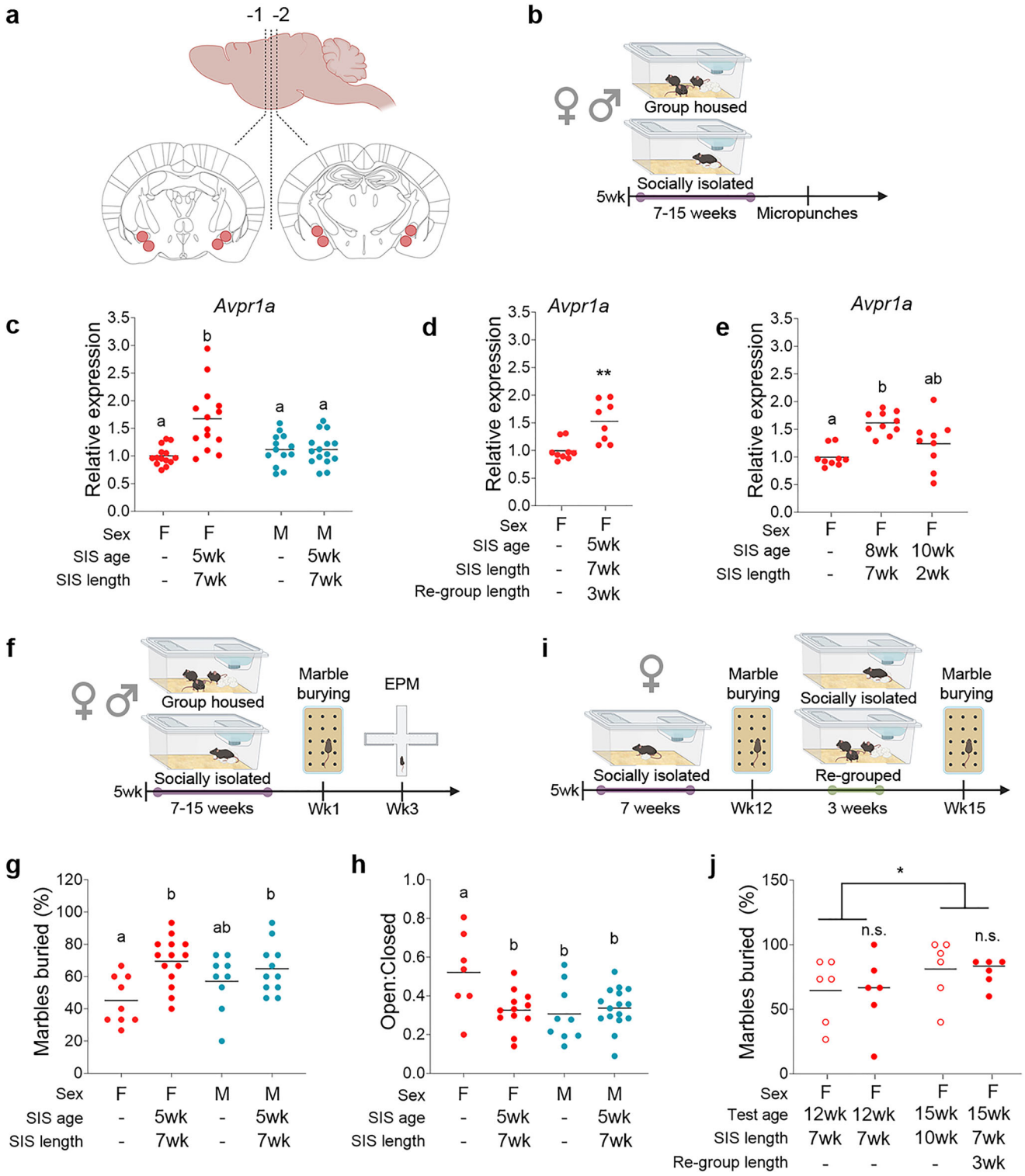

Avpr1a decreased marble burying and increased the time spent in the open arms of the EPM in females but not males, with significant interactions between sex and CSIS (Fig. 3e–g). Deletion of *Avpr1a* had no effect on social behaviors, as demonstrated in the social recognition assay in females (Supplementary Fig. 4a–c). Similar to the deletion of both *Avpr1a* alleles from homozygotes, the deletion of a single copy from $Avpr1a^{Flox/WT}$ heterozygotes decreased marble burying in females in a sex-specific manner, but it did not affect behavior in the EPM (Supplementary Fig. 4d–g). In summary, CSIS-induced adaptations in anxiety-related behaviors require *Avpr1a* in a sex dependent manner. Marble burying is most sensitive to this pathway, as deletion of even one copy of the gene was sufficient to block this behavior, while effects in the EPM were only observed when both copies were lost.

We next asked whether acute blockade of central AVPR1A is sufficient to reverse CSIS-induced anxiety-related behaviors. SRX246 is a selective AVPR1A antagonist that can cross the blood-brain barrier[27] and has been tested in several Phase II clinical trials. We compared the effects of SRX246 (2 mg/kg, i.p.) and an AVPR1A antagonist that cannot cross the blood brain barrier (SR49059, 2 mg/kg, i.p.) in WT mice that were exposed to CSIS starting post-puberty (5 weeks) (Fig. 3h) or in

Fig. 2 | CSIS increases *Avpr1a* expression and anxiety-related behaviors in females. a Schematic of CeA/MePD micropunches analyzed. **b** Experimental design to assess effects of CSIS vs. group housing from 5 weeks of age for ≥7 weeks in WTs on *Avpr1a* expression in the CeA/MePD. **c** CSIS increased *Avpr1a* in females but not males (group $P = 0.0012$, sex $P = 0.0272$, interaction group*sex $P = 0.0012$, $n = 13$ control females, $n = 14$ CSIS females, $n = 13$ control males, $n = 15$ CSIS males). **d** *Avpr1a* in females remained elevated after re-grouping for 3 weeks ($P = 0.0025$, $n = 9$). **e** Initiating 7 weeks of CSIS at 8 weeks of age increased *Avpr1a* in females, but exposure to 2 weeks of isolation from 10 weeks of age did not ($P = 0.0011$, $n = 9$ control females, $n = 10$ 7-wk SIS females, $n = 9$ 2-wk SIS females). **f** Experimental design to assess the effect of CSIS vs. group housing on anxiety-related behaviors in WTs. **g**, **h** CSIS increased marble burying (**g**) and time spent in the center of the elevated plus maze (EPM) (**h**) in females and not males (marble burying: group $P = 0.0020$, sex $P = 0.4645$, group*sex $P = 0.0969$, $n = 9$–14; EPM: group $P = 0.1$, sex $P = 0.0214$, group*sex $P = 0.0102$, $n = 9$ control females, $n = 14$ CSIS females, $n = 9$ control males, $n = 11$ CSIS males). **i** Experimental design to assess effects of re-grouping females for 3 weeks after exposure to CSIS on anxiety-related behaviors. **j** Re-grouping females did not reduce marble burying (group $P = 0.8702$, age $P = 0.0307$, group*age $P = 0.9509$, $n = 6$). Two-way ANOVA (with RM for marble burying) and Tukey's multiple comparisons were used in (**c**, **g**, **h**, **j**). Two-tailed Mann-Whitney test used in (**d**). Kruskal-Wallis test and Dunn's multiple comparisons in (**e**). Different letters denote significant differences. n denotes the number of mice per group. Schematics in (**a**), (**b**), (**f**) and (**i**) were generated with BioRender icons[49].

young adulthood (8 weeks) (Supplementary Fig. 5a). SRX246 decreased marble burying in females and not males, regardless of the age of CSIS initiation, but there was no interaction between sex and CSIS; SR49059 had no effect (Fig. 3i and Supplementary Fig. 5a). The effect of SRX246 in the marble burying assay was dependent on CSIS, as it did not change behavior in group housed females (Supplementary Fig. 5b). SRX246 also increased time in the open arms of the EPM in females in a sex-dependent manner, independent of the age of CSIS onset (Fig. 3j and Supplementary Fig. 5a). In contrast, water intake was not affected (Supplementary Fig. 5c). The effect of SRX246 on marble burying in CSIS females was specific to AVPR1A, as injections of AVPR1B (SSR149415, 2 mg/kg, i.p.) and OXR (β-Mercapto-β,β-cyclopentamethylenepropionyl1,O-Me-Tyr2,Orn8-Oxytocin, 2 mg/kg, i.p.) antagonists did not affect behavior in females or males (Supplementary Fig. 5d). In summary, chronic and acute inhibition of AVPR1A reduce anxiety-related behaviors in the EPM and marble burying tests in females in a context (i.e., CSIS)-dependent manner. With the exception of the effect of SRX246 on marble burying, the effects were sex specific.

Circuits downstream of AVPR1A^{CeA} neurons

We identified downstream targets of AVPR1A^{CeA} neurons that could mediate the effects of CSIS on anxiety-related behaviors. We first performed anterograde tracing by injecting *Avpr1a*-Cre mice with AAV-DIO-Synaptophysin-mCherry in the CeA and quantified the synaptic boutons in all mCherry-positive regions throughout the brain in both sexes (Fig. 4a–d and Supplementary Fig. 6a, c). In females, the most prominent projection sites were the MeA, supraoptic nucleus (SON), DLS, subbrachial nucleus (SubB), lateral preoptic area (LPOA), basomedial amygdala (BMA), nigrostriatal tract (ns), mesencephalic reticular formation (mRT), bed nucleus of the stria terminalis (BNST), and the shell of the nucleus accumbens (NAcc Shell) (Fig. 4d–f and Supplementary Fig. 6d–f). The DLS was the only region with significantly more projections in females than males (Fig. 4d and Supplementary Fig. 6c). This likely does not stem from differences in the number of AVPR1A^{CeA} neurons infected with this viral serotype, as injections of a serotype-matched GFP control virus labeled similar numbers of cells in females and males (Supplementary Fig. 6b).

Next, we examined whether chemogenetic inhibition of AVPR1A^{CeA} → DLS circuits is sufficient to block CSIS-induced behavioral adaptations (Supplementary Fig. 7a). We performed sequential bilateral injections of two viruses in *Avpr1a*-Cre mice exposed to CSIS: first, a retrograde AAV-DIO-Flp in the DLS, then three weeks later, an AAV-fDIO-DREADDGi-mCherry in the CeA (Supplementary Fig. 7b). mCherry was expressed in the CeA in only half of the mice injected ("hits") (Supplementary Fig. 7c); the remainder did not express mCherry anywhere in the brain ("missed") and served as controls. Chemogenetic inhibition of AVPR1A^{CeA} → DLS circuits decreased marble burying and increased the time spent in the open arms of the EPM in females but not in males (Supplementary Fig. 7d, e); the interaction between sex and CSIS was significant in the marble burying test and trended toward significance in the EPM. This supports the idea that the DLS mediates some of the sex-specific effects of AVPR1A^{CeA} neurons in the context of CSIS.

We also explored the possibility that AVPR1A^{CeA} neurons that project to the DLS also send collaterals to other targets, which could contribute to the effects of chemogenetic activation. To this end, we performed monosynaptic rabies tracing by first injecting AAV-EF1a-DIO-HTB in the CeA of *Avpr1a*-Cre mice. 3 weeks later, we injected EnvA-G-Deleted-Rabies-mCherry in the DLS. After 7 days, we quantified mCherry expression across the brain (Fig. 4g–i and Supplementary Fig. 8a). We identified collaterals projections in the SubB, mRT, BNST, periaqueductal gray area (PAG), and the paraventricular nucleus of the hypothalamus (PVH, Supplementary Fig. 8b–e). We then utilized an optogenetic approach to determine whether acute inhibition of AVPR1A^{CeA} → DLS projections, without affecting collaterals, is sufficient to reverse the effects of CSIS to enhance anxiety-related behaviors in *Avpr1a*-Cre females mice exposed to CSIS (Fig. 4j–l). We injected an AAV-DIO-NpRH-EYFP or AAV-DIO-EYFP viral construct in the CeA of *Avpr1a*-Cre mice and implanted a light cannula above the DLS. Marble burying behavior was suppressed in the "lights on" as compared to the "lights off" condition in *Avpr1a*-Cre females expressing the inhibitory opsin, NpHR, but not in control mice injected with AAV-DIO-EYFP viral construct (Fig. 4m). Optogenetic inhibition of AVPR1A^{CeA} → DLS projections increased the time spent in the open arms of the EPM (Fig. 4n) in the NpHR group compared to the control group injected with AAV-DIO-EYFP viral construct.

MePD is a key source of AVP to AVPR1A^{CeA}

To identify potential sources of AVP to the CeA, we used complementary viral tracing approaches. We generated an *Avp*-Flp mouse line that we crossed to a GFP reporter line (*Avp*-Flp::GFP) and used smFISH to confirm that *Gfp* transcript was detected in ~95% of *Avp*-expressing cells (Supplementary Fig. 9a, b). First, we identified AVP neurons that project in the vicinity of AVPR1A^{CeA} neurons by injecting *Avp*-Flp::GFP mice with a retrograde AAV-fDIO-mCherry in the medial aspect of the CeA (Fig. 5a and Supplementary Fig. 9c). We observed robust labeling in the MePD, thalamic reticular nucleus (TRN), SON, anteroventral aspect of the MeA (MeAV) in both sexes, and a few cells in the suprachiasmatic nucleus (SCN), PVH, DLS, and BNST (Fig. 5b and Supplementary Fig. 9e–k). We focused on the MePD, because it was the only site labeled in 100% of females and males (Supplementary Fig. 9d). To determine whether AVP^{MePD} neurons send direct projections to AVPR1A^{CeA} neurons, we crossed *Avp*-Flp::GFP and *Avpr1a*-Cre::tdTOM mouse lines. We detected GFP-positive AVPergic fibers at the border between the MePD and medial aspect of the CeA; however, only a few fibers were detected within the CeA, and they were not in close contact with AVPR1A^{CeA} neurons (Fig. 5c and Supplementary Fig. 10a).

AVP can diffuse over 100-150μm to modulate neuronal activity in the absence of a direct, wired connection[28,29]. Therefore, we examined whether AVP produced in the MePD contributes to CSIS-induced anxiety-related behavioral adaptations. We utilized a virus-based CRISPR approach (AAVs expressing Cas9 and an *Avp* guide RNA vs. a

https://doi.org/10.1038/s41467-025-64742-y

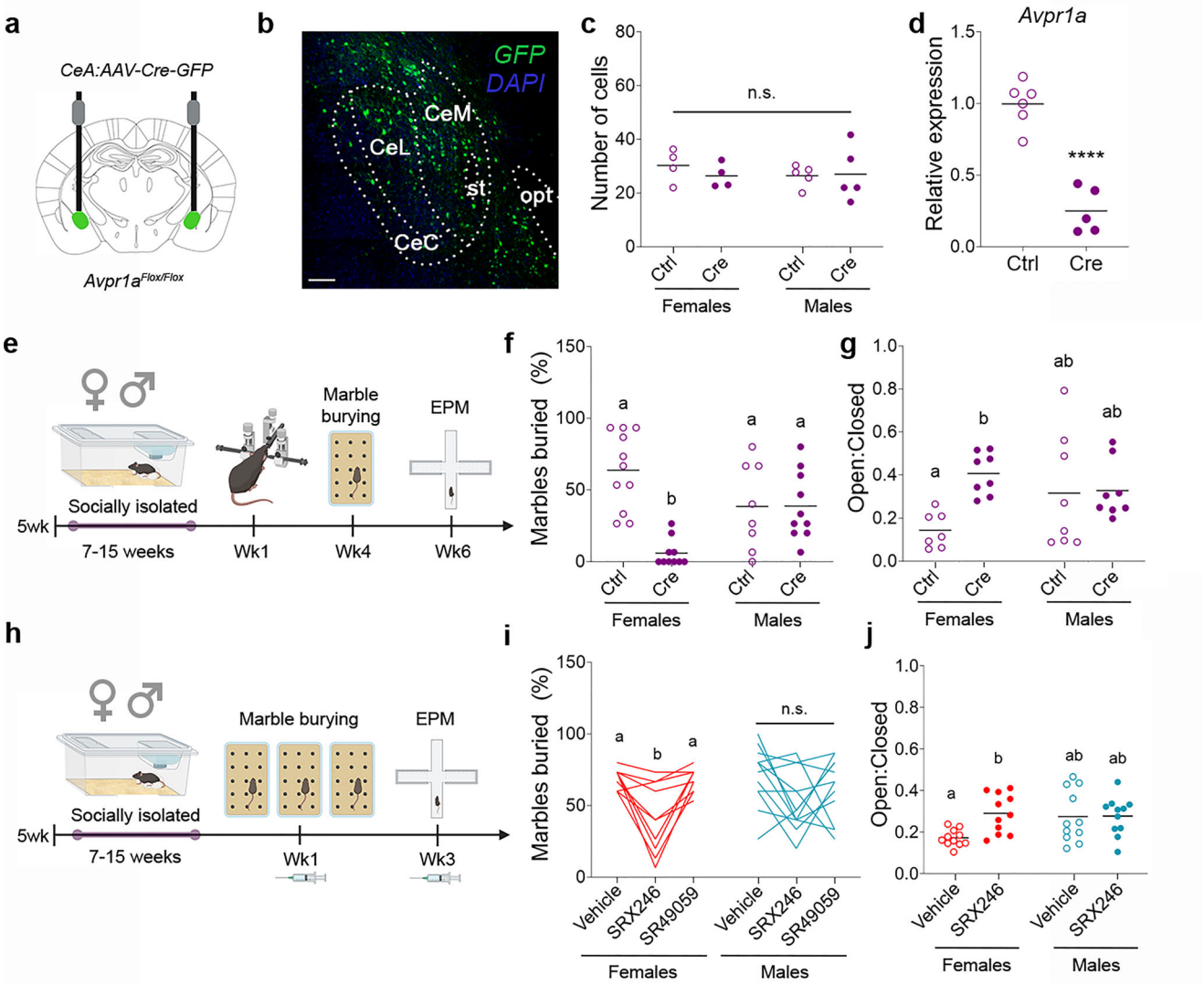

Fig. 3 | AVPR1A in the CeA is necessary for CSIS-induced anxiety-related behaviors in females. a Schematic of intra-CeA injections in *Avpr1a*$^{Flox/Flox}$ mice used to generate conditional knockouts (cKOs). **b** Representative GFP expression in the CeA. **c** Similar number of GFP-expressing CeA neurons between control and Cre viruses and between sexes (group $P = 0.6584$, sex $P = 0.6804$, interaction group*sex $P = 0.5333$, n = 4 females, n = 5 males). **d** Diminished *Avpr1a* in the CeA/MePD in *Avpr1a*$^{Flox/Flox}$ injected with Cre versus control virus ($P = < 0.0001$, $n = 6$ control, $n = 5$ Cre). **e** Experimental design to assess CSIS-induced anxiety-related behaviors in cKOs. **f**, **g** Decreased marble burying (**f**) and increased time in the open arm of the EPM (**g**) in females but not males (marble burying: group $P = 0.0006$, sex $P = 0.6300$, interaction group*sex $P = 0.0005$, $n = 11$ control females, $n = 10$ Cre females, $n = 8$ control males, $n = 10$ Cre males; EPM: group $P = 0.0283$, sex $P = 0.4419$, interaction group*sex $P = 0.0430$, $n = 7$ control females, $n = 8$ Cre females, $n = 8$ control males, $n = 8$ Cre males). **h** Experimental design to assess CSIS-induced anxiety-related behaviors following pharmacological blockade of AVPR1A. **i**, **j** SRX246 reduced marble burying (**i**) and increased time in the open arm of the EPM (**j**) in females and not males exposed to CSIS, while SRX49059 had no effect (marble burying: group $P = 0.0003$, sex $P = 0.6348$, interaction group*sex $P = 0.2733$, $n = 10$ females, $n = 12$ males; EPM: group $P = 0.0397$, sex $P = 0.1204$, interaction group*sex $P = 0.046$, $n = 11$ vehicle-injected females, $n = 11$ SRX246-injected females, n = 10 vehicle-injected males, $n = 11$ SRX246-injected males). Two-way ANOVA used in (**c**). Two-way ANOVA (with RM for marble burying) and Tukey's multiple comparisons used in (**f**–**g**) and (**i**, **j**). Unpaired two-tailed t-test used in (**d**). Different letters denote significant differences. n denotes the number of mice per group. Scale bar represents 100 µm. Schematics in (**e**) and (**h**) generated with BioRender icons[49].

scrambled control guide RNA) to achieve a > 50% reduction in *Avp* in the MePD of WT mice exposed to CSIS, which we confirmed with RT-qPCR (Fig. 5d–f). Diminished *Avp* in the MePD led to reduced marble burying and increased time spent in the open arms of the EPM in females but not males, but there was no interaction between sex and CSIS (Fig. 5f–h). Together, these data provide evidence that AVP in the MePD is required for the effect of CSIS on anxiety-related behaviors but is not a driver of sex-specificity.

ERα in AVP^{MePD} boosts sex specificity

The MePD is a sexually dimorphic brain region that regulates sex-specific behaviors, in part through ERα signaling[30,31]. We confirmed that >90% of AVP^{MePD} neurons co-expressed ERα by immunohistochemistry in the *Avp*-Flp::GFP reporter line (Supplementary Fig. 10b, c). We used an intersectional approach to exclusively delete *Esr1*, the gene encoding ERα, from AVP^{MePD} neurons, which represent a very small subset of all ERα-positive neurons in the MePD (Supplementary Fig. 10b). We generated *Avp*-Flp::*Esr1*$^{flox/flox}$ mice and injected them with AAV-fDIO-Cre or a control virus in the MePD (Fig. 5i, j). We confirmed the specific deletion of *Esr1* in AVP^{MePD} neurons by smFISH (Fig. 5k). Deletion of *Esr1* from the AVP^{MePD} neurons in the context of CSIS decreased marble burying in females in a sex-dependent manner (Fig. 5l). Females also exhibited a trend toward increased time spent in the open arm of the EPM, but this did not reach significance ($P = 0.06$)

https://doi.org/10.1038/s41467-025-64742-y

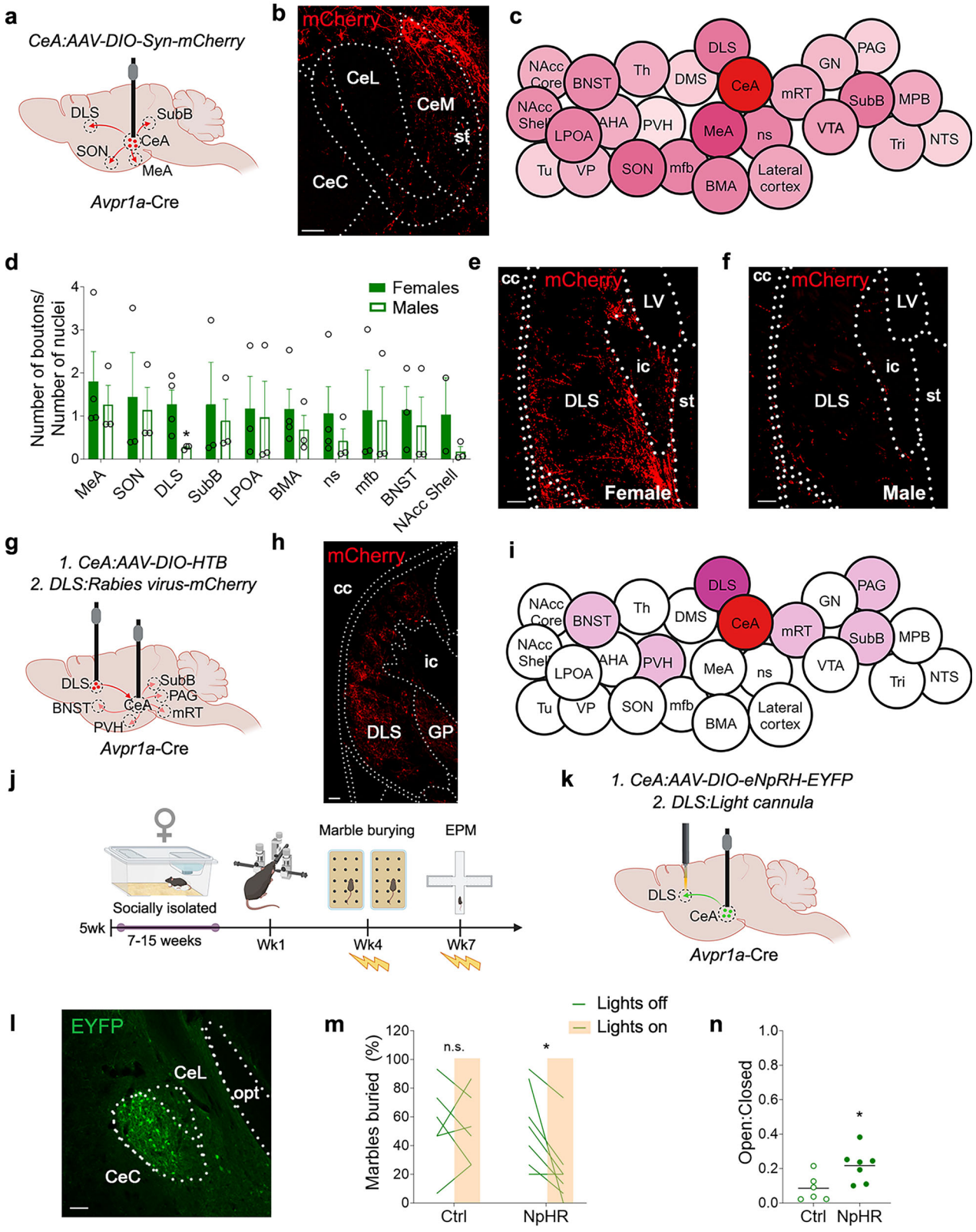

(Fig. 5m). These data support the idea that estrogen signaling through ERα in AVP^{MePD} neurons contributes to increased sensitivity of females to CSIS.

Discussion

Sex differences in responsiveness to social stress in adulthood are highly conserved across species, with females more sensitive to isolation[14,32,33]. We identified an AVP^{MePD} → AVPR1A^{CeA} → DLS circuit that mediates these effects.

Anxiogenic AVPR1A^{CeA} circuits are distinct

Amygdala activation is associated with anxiety in humans[34] and exogenous stimulation of several subpopulations of CeA neurons is sufficient to induce anxiety-related behaviors in rodents. However, the

Fig. 4 | AVPR1A^{CeA} → DLS circuits mediate behavioral adaptations to CSIS in females. a Schematic of viral injection for anterograde tracing from AVPR1A^{CeA} neurons. **b** Representative expression of the viral mCherry reporter in the CeA ($n = 7$). **c** Overview of AVPR1A^{CeA} neuronal projections in females, with colors corresponding to the heatmap shown in Supplementary Fig. 6. **d** DLS is the only region with a higher density of synaptic boutons from AVPR1A^{CeA} neuronal projections in females compared to males ($P = 0.04818$, $n = 2$ female NAcc, $n = 3$ female SON, SubB, LPOA, mfb, BNST, $n = 4$ female MeA, DLS, BMA, ns, $n = 3$ males). **e**, **f** Representative expression of the viral mCherry reporter in the DLS in females (**e**) and males (**f**). **g** Schematic of viral injections for rabies tracing of AVPR1A^{CeA} → DLS collateral projections. **h** Representative expression of the viral mCherry reporter in the DLS ($n = 5$). **i** Overview of AVPR1A^{CeA} neuronal projections with collaterals to the DLS. **j** Experimental design to assess the effect of optogenetic inhibition of AVPR1A^{CeA} → DLS projections on CSIS-induced anxiety-related behaviors. **k** Schematic of viral injection into the CeA and fiber placement in the DLS of *Avpr1a*-Cre females. **l** Representative expression of the viral EYFP reporter in the CeA ($n = 13$). **m**, **n** Exposure to light with a wavelength of 590 nm to inhibit AVPR1A^{CeA} → DLS projections expressing halorhodopsin (NpHR), but not control virus, reduced marble burying (**m**) and increased time spent in the open arms of the EPM (**n**) in females exposed to CSIS (marble burying: Ctrl $P = 1$, NpHR $P = 0.0355$; EPM: $P = 0.0205$, $n = 6$ controls, $n = 7$ NpHR). Data are presented as means +/− SEM in (**d**). Multiple unpaired *t*-tests were used in (**d**). Paired Wilcoxon signed rank test with continuity correction was used in (**m**). Unpaired two-tailed *t*-test was used in (**n**). n denotes the number of mice in each group. Scale bars represent 100 µm. Schematics in (**a**), (**g**), (**j**) and (**k**) were generated using BioRender icons[49].

neuroanatomical and molecular properties of AVPR1A^{CeA} neurons suggest they are distinct from other anxiogenic subpopulations of CeA neurons that have been described. We analyzed a spatial transcriptomic dataset from the male mouse amygdala[35] and determined that *Avpr1a* expression is largely restricted to two GABAergic neuronal subtypes in the medial aspect of the CeA (GABA-20 and −21), consistent with the distribution of the *Avpr1a*-Cre::tdTomato lineage trace. Together, the *Avpr1a*+ subpopulations account for 4.4% of all GABAergic neurons in the CeA. There is virtually no co-expression of *Avpr1a* with either *Tac2* or *Chrh1* or (0–2 cells per subpopulation), molecular markers for other anxiogenic CeA neuronal subpopulations[36,37].

AVPR1A^{CeA} neurons project most strongly to sites in the amygdala, forebrain, and midbrain reticular formation that regulate goal-directed behaviors, habit formation, and arousal. This contrasts with the remainder of the CeA, which sends descending projections to midbrain and brainstem circuits that regulate appetitive, aversive, and defensive behaviors[38]. In addition, our viral tracing data supports the idea that AVPR1A^{CeA} neurons are distinct from anxiogenic CeA→basolateral amygdala circuits[39]. Chemogenetic inhibition of CeA→BNST circuits prevents anxiety-related behavioral adaptations in the context of sepsis[40]. Since they did not target their manipulations to a genetically defined subpopulation of neurons, it is possible that some AVPR1A^{CeA} neurons contributed to this effect. These observations highlight the importance of identifying neurons that respond to different types of endogenous stressors rather than "anxiety-related" behavioral outcomes. Whereas the AVPR1A^{CeA} system is not engaged by overcrowding or repeated restraint, it is possible that it is activated by other stressors that contribute to anxiety-related behaviors in females and/or males. These signals could be conveyed by AVP neurons in the TRN, SON, MeAV, or SCN that project to the AVPR1A^{CeA} system in a sex-independent manner.

AVPR1A drives sex-specificity in CSIS

The AVPR1A system is upregulated in the context of restricted social interactions, but the specific brain circuits and behaviors affected are sex- and age-dependent. Imposing CSIS at weaning led to increased social (aggressive) behaviors that were associated with changes in AVPR1A binding in the LH, DG, and BNST, while anxiety-related behaviors and binding in the CeA were not altered[17]. Here, we show that post-pubertal CSIS exclusively induces *Avpr1a* expression in the CeA in females. Not only is the timing of the onset of social isolation critical to engage AVPR1A circuits in the amygdala, but so is the duration of exposure, as we found that *Avpr1a* expression was not significantly increased in females singly housed for 2 weeks. This is reminiscent of our previous observation that females are preferentially sensitive to longer (7 weeks vs. 2 weeks) periods of social isolation in a novelty-suppressed feeding paradigm[14]. Genetic[41] or pharmacological (this study) blockade of AVPR1A function does not alter anxiety-related behaviors in group-housed females. Together, these observations are consistent with the idea that effects of AVPR1A signaling in the CeA on behavior are relatively specific to contexts when it is activated over baseline levels, such as CSIS.

ERα signals in upstream AVP^{MePD} neurons

AVP neurons are distributed throughout the brain, and their projection patterns are notable for their high degree of sexual dimorphism and responsiveness to gonadal hormones[42], supporting the idea that AVP plays an important role in mediating sex differences in behavior. Based on tracing studies in male rats, it has been assumed that the PVH is the primary source of AVP to the CeA[18]. We did not observe robust AVP projections from the PVH in males or females, consistent with studies in humans[43]. Instead, we identified the MePD as a major source of AVP to the medial-most portion of the CeA. AVP^{MePD} neurons projected in the vicinity of AVPR1A^{CeA} neurons in both males and females, but did not contact them directly, consistent with a paracrine mode of release of AVP^{MePD} neurons[28], although identifying the mode of signaling is an important area for future research. We also noted that knockdown of *Avp* in the MePD produced a less robust response than deletion of *Avpr1a* in the CeA, raising the possibility that other populations of AVP populations that project to AVPR1A^{CeA} neurons (e.g., TRN and SON) also affect anxiety-related behaviors.

In contrast to loss-of-function manipulations of AVPR1A signaling or projections to the DLS, which were highly dependent on sex, there was no interaction between sex and stress for KD of *Avp* in the MePD. Regulation of AVP expression and release from the MePD by gonadal hormones is well-documented, but studies were almost exclusively conducted in males[42]. AVP^{MePD} neurons account for only 0.38% of all *Esr1*-expressing neurons in the MeA[35]. And yet, loss of *Esr1* from AVP^{MePD} neurons decreased some of the CSIS-induced behavioral adaptations in females, consistent with a sex-specific role for ERα signals in promoting AVP expression and or release.

Sources of sex specificity

Gain of function approaches that pharmacologically or chemogenetically activate AVPR1A^{CeA} circuits induce anxiety-related behaviors in both sexes. However, genetic, pharmacological, chemogenetic, and optogenetic loss of function approaches support the idea that in the context of CSIS this system is only engaged in females. We identified three different substrates for sex-specific influences: 1) engagement of the AVPR1A pathway in the CeA by CSIS; 2) density of projections to the DLS; and 3) ERα signaling in AVP^{MePD} neurons. CSIS may activate anxiogenic circuits outside CeA in males that contribute to anxiety, albeit to a lesser extent. Similarly, it is possible that AVP → AVPR1A circuits in the amygdala are preferentially activated in males in other contexts, such as social defeat stress in adulthood[44].

Potential therapeutic implications

Females are more sensitive to social exclusion and loneliness[13,45], which has been implicated in the etiology of anxiety disorders[46]. There is empirical support for the use of pharmacotherapies in patients with

https://doi.org/10.1038/s41467-025-64742-y

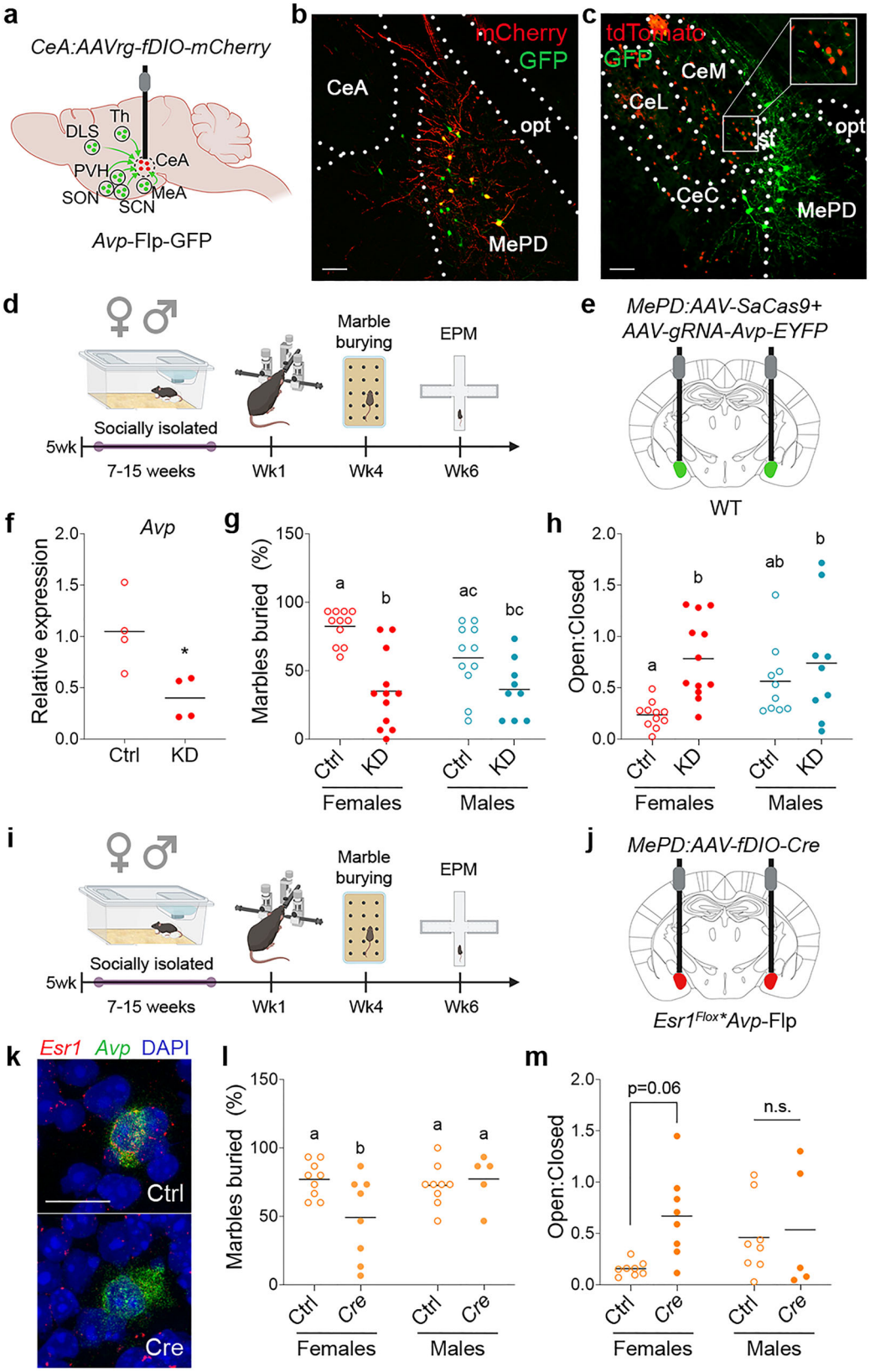

anxiety disorders, but many do not respond to treatment[47]. We found that the effects of genetic or pharmacological loss of AVPR1A function to reduce anxiety-related adaptations are influenced by sex. And yet, clinical trials with AVPR1A antagonists, such as SRX246, have almost exclusively explored aggression and other behavioral endpoints in males. Since we found that SRX246 did not affect anxiety-related behaviors in males or group-housed females, consideration of sex and perceived loneliness should be used to identify people who are more likely to respond to treatment.

In conclusion, our studies are consistent with the growing call to develop therapeutics that target the etiology of a psychiatric disorder, rather than its symptoms.

Fig. 5 | ERα neurons in the MePD are a source of AVP. a Schematic of intra-CeA injections in *Avp*-Flp::GFP mice to identify sources of AVP. **b** Co-expression of the viral mCherry reporter in GFP-labeled AVP^{MePD} neurons ($n = 2$). **c** GFP+ fibers from AVP^{MePD} neurons project toward tdTomato+ $AVPR1A^{CeA}$ neurons in *Avpr1a*-Cre::td-Tomato::*Avp*-Flp::GFP mice. **d** Experimental design to assess effects of MePD *Avp* knockdown (KD) on CSIS-induced anxiety-related behaviors. **e** Schematic of intra-MePD injections in WTs. **f** Reduced *Avp* in the CeA/MePD ($P = 0.0219$, $n = 4$). **g**, **h** *Avp* KD in the MePD reduced marble burying (**g**) and increased time in the open arms of the EPM (**h**) in females but not males exposed to CSIS (marble burying: group $P = < 0.0001$, sex $P = 0.1257$, interaction group*sex $P = 0.0877$; EPM: group $P = 0.0045$, sex $P = 0.2467$, interaction group*sex $P = 0.1309$, $n = 11$ control females, $n = 12$ KD females, $n = 11$ control males, $n = 9$ KD males). **i** Experimental design to assess effects of *Esr1* deletion from AVP^{MePD} neurons on CSIS-induced anxiety-related behaviors. **j** Schematic of viral injection in $Esr1^{Flox/Flox}$::*Avp*-Flp::GFP females. **k** Reduced *Esr1* in *Avp*-expressing MePD neurons in Cre-injected females ($n = 4$ Cre, $n = 3$ control). **l**, **m** *Esr1* knockout from AVP^{MePD} neurons reduced marble burying (**l**) and increased time in the open arms of the EPM (**m**) in females and not males (marble burying: group $P = 0.1335$, sex $P = 0.1243$, interaction group*sex $P = 0.0381$, $n = 9$ control females, $n = 8$ Cre females, $n = 9$ control males, n = 5 Cre males; EPM: group $P = 0.0543$, sex $P = 0.5661$, interaction group*sex $P = 0.1454$, n = 8 females and control males, n = 5 for Cre males). Unpaired two-tailed *t*-test used in (**f**). Two-way ANOVA (with RM for marble burying) and Tukey's multiple comparisons used in (**g**), (**h**), (**l**) and (**m**). Different letters denote significant differences. n denotes the number of mice per group. Scale bars represent 100 µm in (**b**) and (**c**), and 25 µm in (**k**). Schematics in (**a**), (**d**) and (**l**) were generated with BioRender icons[49].

Methods

Animals

All animals were maintained on a 12 h/12 h light/dark cycle (7 am lights on), with ad libitum access to food and water, unless stated otherwise. C57BL/6 J mice (Jax strain #000664, WT) were used for behavioral, mRNA expression, CRISPR knockdown, and pharmacological studies. The *Avpr1a-Cre* line was generated by the Molecular Genetics Core at the University of Michigan by inserting the P2A-Cre transgene in frame with *Avpr1a* using CRISPR-mediated gene editing techniques and was used for histology, tracing, chemogenetic, and optogenetic studies. The *Avpr1a-Cre* mouse line was crossed onto the 6.Cg-Gt(ROSA) 26Sorm9(CAG-tdTomato)Hze/J reporter line (Ai9, Jax strain #007909). B6.129P2- Avpr1atm1Dgen/J mice (Jax strain #005776, $Avpr1a^{-/-}$) were used for pharmacological studies. $Avpr1a^{Flox}$ and *Avp*-Flp lines were generated by Cyagen Biosciences (Santa Clara, CA) and provided by the Dölen laboratory. Cre-dependent *Avpr1a* knockout mice ($Avpr1a^{Flox}$) were generated by inserting LoxP sites flanking exon 1 of the m*Avpr1a* gene. The targeting vector was generated by PCR using BAC clones RP24-352P7 and RP24-268P17 from the C57BL/6 J library as template. *Avp*-Flp mice were generated by replacing the stop codon in exon 3 of the endogenous m*Avp* gene with a 2A-Flp construct. The *Avp*-Flp line was crossed onto the Gt(ROSA)26Sortm1.2(CAG-EGFP)Fsh/Mmjax mouse line (Jax strain #32038), and onto the B6(Cg)-Esr1tm4.1Ksk/J mouse line (Jax strain # 032173). All procedures were performed within the guidelines of the Institutional Animal Care and Use Committee (IACUC) at the Columbia University Health Science Division and the New York State Psychiatric Institute.

Stresses

Chronic social isolation. Mice were either housed in cages of 4 (group-housed control) or singly housed at 5 weeks of age for at least 7 weeks in standard cages. Additional control groups included mice socially isolated at 5 weeks of age for 7 weeks and regrouped at 12 weeks for 3 weeks, and mice isolated at 8 weeks of age for 7 weeks, or at 10 weeks of age for 2 weeks. For the re-grouping experiment, marble burying behaviors in CSIS females at 12 weeks were used to assign the mice into matched groups of socially isolated and re-grouped females.

Overcrowding. Mice were either housed in cages of 4 (group-housed control) or in cages of 8 (overcrowded) at 5 weeks of age for 7 weeks.

Repeated restraint. At 12 weeks of age, animals were restrained in well-ventilated 50 ml tubes and left undisturbed for 1 h on 5 consecutive days. Mice were euthanized at the end of the 5^{th} day.

Behavioral assays

All behavioral assays were performed after lights out (7 pm) after 7 to 12 weeks of social isolation. Marble burying and EPM assays were performed by the Zeltser lab in Columbia University barrier facilities, while all other neurobehavioral tests were performed by the Bath laboratory in New York State Psychiatric Institute barrier facilities.

Marble burying. Animals were tested under red lighting. Standard cages were filled with fresh bedding to a depth of 2.5 cm and 15 marbles were evenly spaced across the bedding. Animals were placed in the cage for 30 min and allowed to ambulate freely. At the end of the assay, the number of marbles buried was estimated visually. A marble was considered buried if at least 3/4 of its surface was covered by the bedding.

Elevated plus-maze (EPM). Animals were habituated in the dark for 30 min and tested under low lighting. The apparatus consisted of a platform elevated 30 cm above the floor with four perpendicular arms; two arms were enclosed by 20 cm high walls and two arms were open. At the beginning of the test, mice were placed into the center zone facing the open arms and allowed to move freely for 15 min while beam breaks were recorded in each arm by the MED-PC V 64 bit Software (Med Associates).

Sucrose preference. Animals were acclimated to two identical bottles (Nalgene) filled with either tap water or 1% sucrose solution (Fisher Scientific) for three days. Mice and bottles were weighed every day at the beginning of the dark cycle. The two bottles were switched on each day.

Open field. Animals were habituated in the dark for 30 min and tested two at a time in the open field (18 in x 24 in x 14 in) for 10 min (150 lux in the center). The behavior was video-tracked using Ethovision software.

Novel object recognition. Animals were habituated in the dark for 30 min and tested two at a time in the chamber (25–30 lux in the center). *Familiarization*: Each chamber contained two identical objects and animals were allowed to explore the objects for 5 min. *Testing*: Both objects were replaced but the identity of one remained the same. Change sides were counterbalanced. Animals were allowed to explore the objects for 5 min. Preference index was calculated as [interaction time novel/total interaction time].

Rotarod. Animals were habituated in the dark for 15 min tested in the dark, five at a time, for motor performance on an accelerating rotarod (4–40 RPM) for five runs of 5 min with 1 min between each run.

Forced swim test. Animals were habituated in the dark for 30 min and tested five at a time under low lighting. Mice were placed into a 2000 mL beaker filled to 1600 mL with 23 °C water for 6 min. The behavior was video tracked using Ethovision software with a mobility threshold of 3% for immobility. Time spent immobile was binned for each minute and the average of the last 4 min of immobility was compared across groups.

Social recognition. Animals were tested under red lightning. Singly housed WT females were housed in their home cages. On day one, a novel female mouse was introduced into the cage, and behaviors were recorded using ANY-maze software. Time spent sniffing the novel individual was scored manually. On day 2, the novel individual was re-introduced to the same cage, and time spent sniffing was recorded and scored manually.

mRNA extraction

Mice were anesthetized after 7 pm (Avertin, i.p., 0.32 ml/10 g of 2.5% solution, Sigma Aldrich; or isoflurane 5% isoflurane/1 L O_2/min) and euthanized by decapitation. The CeA and MeD were micro-dissected from two 0.5 mm slices of the brains at bregma −1.0 mm and −2.0 mm with the EMS-Core Sampling Tool (EMS) in two punches of 0. 5 mm diameter. Snap-frozen tissues were homogenized and mRNA was extracted using the RNeasy Micro Kit (Qiagen).

qPCR

cDNA was generated from 50 to 200 ng of total RNA by reverse transcription using the SuperScript™ IV VILO™ Master Mix (Invitrogen). RT-qPCR was performed with the QuantStudio 5 RT-qPCR system, Design & Analysis software, and TaqMan Fast Advanced master mix (Applied Biosystems). Expression was normalized using the housekeeping gene *Glyceraldehyde-3-phosphate dehydrogenase* (*Gapdh*). TaqMan assays (Applied Biosystems) included: *Gapdh*, Mm00434129_m1; *Avpr1a*, Mm00444092_m1; and *Avp*, Mm01271704_m1. Relative quantification of gene expression was calculated using the 2-ΔΔCt formula (Schmittgen TD, and Livak KJ. Analyzing real-time PCR data by the comparative C(T) method. *Nat Protoc*. 2008;3(6):1101-8).

Perfusion and immunohistochemistry

Mice were deeply anesthetized (Avertin, i.p., 0.32 ml/10 g of 2.5% solution) and transcardially perfused with iced-cold physiological saline followed by 4% paraformaldehyde. Mice were decapitated, and brains were extracted and post-fixed in 4% paraformaldehyde overnight at 4 °C. Brains were then cryoprotected in 30% sucrose, frozen at −80 °C, cut into four series of 30 μm-thick sections across the brain, and processed for free-floating immunohistochemistry. Primary antibodies used were rabbit anti-DsRed (1:500; #632496, Takara), rat anti-mCherry (1:1000, # 16D7, Invitrogen), goat anti-cFos (1:1000, #PA1-18329, Invitrogen), and sheep anti-GFP (1:1000; # 4745-1051, Biorad). Secondary antibodies used were donkey anti-rabbit (#A-31572, Invitrogen), donkey anti-rat IgG-Alexa594 (#A-11007, Invitrogen), donkey anti-goat IgG-Alexa488 (#A32814, Invitrogen), donkey anti-sheep IgG-Alexa488 (#A-11015, Invitrogen). Free-floating sections were mounted on microscope slides, and immunofluorescence was visualized with a 4',6-diamidino-2-phenylindole (DAPI) counter stain using a Zeiss LSM 710 confocal microscope (Zeiss) or an Aperio VERSA 8 Scanning System.

Histology

Counts were performed on one of the four series of 30 μm sections.

Cell counts. Boundaries of each region were delimited using a mask overlay generated from the Allen Brain Atlas. Counts were performed manually by an investigator blinded to the conditions. An average of 2–3 sections was calculated for each region for each mouse.

Bouton counts. Brain regions expressing mCherry were delimited using the Qupath software from whole-slide scans. The density of boutons was estimated in each region using an automated pipeline generated in ImageJ[48]. Counts were normalized by the number of DAPI-stained nuclei estimated in each region of interest, and an average was calculated from one to ten sections per region.

Stereotaxic surgery

Mice were anesthetized with isoflurane (1–5% isoflurane/1 L O_2/min) and placed on a double-armed stereotaxic frame (Stoelting). For acute viral injections, ophthalmic ointment and analgesics were administered (buprenorphine, 0.1 mg/kg or buprenorphine Ethiqa XR, 3.25 mg/kg, subcutaneous). A craniotomy was made to insert a guide cannula (Model C315G/SPC, Plastics One) to the CeA (1.34 mm posterior, +/−2.4 mm lateral, and 4.5 mm ventral to bregma according to the Paxinos and Franklin mouse brain atlas) or the DLS (1.34 mm posterior, +/−2.95 mm lateral, and 3.7 mm ventral to bregma). The following adeno-associated virus (AAV) viruses were injected: AAV5-hSyn-DIO-hM3Dq-mCherry (Designer Receptors Exclusively Activated by Designer Drugs, DREADD-Gq, titer 6×10^{12} cfu/ml, 250 ul bilateral, #44361, Addgene), AAV5-hSyn-DIO-mCherry (control, titer 6×10^{12} cfu/ml, 250 nl bilateral, #50459, Addgene), AAV5-hSyn-GFP-Cre (titer 3.5×10^{12} cfu/ml, 250 nl bilateral, #6446 C, UNC vector core), AAV5-hSyn-EGFP (titer 4×10^{12} cfu/ml, 250 nl bilateral, #4657D, UNC vector core), AAV8.2-hEF1a-DIO-Synaptophysin-mCherry (titer 2.5×10^{13} vg/ml, 100 nl unilateral, #AAV-RN1, MGH), AAV8.2-EF1a-DIO-Tdtomato-revGFP (titer 1.4×10^{13} vg/ml, 100 nl bilateral, Virovek), AAV2-EF1a-DIO-HTB (titer 1.63×10^{11} gc/mL, GT-AA-072, Salk), AAVrg-Ef1a-fDIO-mCherry (2.2×10^{13} vg/ml, 100 nl unilateral, #114471, Addgene), pAAV(Exp)-CMV-SaCas9 (titer $>2 \times 10^{13}$ vg/ml, 250 ul bilateral, #AAV9SP(VB210611-1334ntv), VectorBuilder), pAAV2gRNA-EGFP (mouse Avp_gRNA#1) (titer $>2 \times 10^{13}$ vg/ml, 250ul bilateral, #AAV9SP(VB210611-1330hbv), VectorBuilder), pAAV(2gRNA)-EGFP (scramble) (titer $>2 \times 10^{13}$ vg/ml, 250 ul bilateral, #AAV9SP(VB210615-1067hym), VectorBuilder), AAV9-EF1a-fDIO-Cre (1.3×10^{13} vg/ml, 100 nl unilateral, #121675, Addgene), AAV5-EF1a-fDIO-mCherry (1×10^{13} vg/ml, 100 nl unilateral, #121675, Addgene), AAVrg-EF1a-DIO-FLPo-WPRE-hGHpA (titer 1.6×10^{13} vg/ml, 250 nl bilateral, #87306, Addgene), AAV-DJ-hSyn-fDIO-hMD4Gi-mCherry (titer 2×10^{13} vg/ml, 250 nl bilateral, #GVVC-AAV-154, Stanford University Gene Vector and Virus Core). EnvA G-Deleted Rabies-mCherry (8.08×10^{8} TU/mL, RbE-04172020-B, Salk) was also used for labeling collaterals of CeA→DLS projections. Injections were performed with a unilateral injector (Model C315I/SPC, Plastics One) attached to a Hamilton syringe (0.5 ml; Hamilton Company) and an infusion pump (KD Scientific #100) at an infusion rate of 50 nL/min. The cannula and injector remained in place for 5 min to prevent backflow. Skull access was then sealed with bone wax (#DYNJBW25, Medline), and the incision was closed with wound clips (#RF7, Braintree Scientific). All experiments were performed at least 3 weeks after injection to ensure maximal viral expression.

For cannulations, ophthalmic ointment and analgesics were administered (buprenorphine, 0.1 mg/kg or buprenorphine Ethiqa XR, 3.25 mg/kg, and carprofen, 5 mg/kg, subcutaneous). For pharmacological experiments, two cannulas (Model C317GS, Plastics One) were placed by drilling holes at the following coordinates: −1.4 mm anteroposterior, +/−2.4 mm lateral, and −4.6 mm ventral to bregma. For optogenetics, one cannula was placed by drilling holes at the following coordinates: 1.34 mm posterior, +/−2.4 mm lateral, and 4.5 mm ventral to bregma. Implants were secured by dental cement and protected with a cap (Model C317DCS, Plastics One). Mice were given one week to recover.

Chemogenetic experiments

Mice were injected with clozapine-N-oxide (CNO, 1.5 mg/kg, i.p., #SML2304, Sigma-Aldrich) 30 min prior to behavioral testing or euthanasia.

Optogenetic experiments

After recovery from the surgery, mice were habituated to the head-fixed optical fiber in their home cage for 30 min for at least two days. Prior to the assays, mice were given 15 min to acclimate to the head-fixed optical fiber in their home cage. For the marble burying assay,

conditions with or without light stimulation (ON: 30 s; OFF: 180 s) were counterbalanced for all of the mice. Since the EPM can only be performed once, two different groups of mice were compared.

Single-molecule fluorescent in situ hybridization (smFISH)

Mice were anesthetized (Avertin, i.p., 0.32 ml/10 g of 2.5% solution) and decapitated. Brains were embedded in OCT (Tissue-Tek) and snap frozen, and coronal cryosections (20 μm) were thaw-mounted onto Superfrost Plus slides (Fisherbrand) prior to storage at −80 °C. smFISH was performed using RNAscope Fluorescent Multiplex Kit (ACDBio). Probes used included: *Avpr1a* (#418061), *Solute carrier family 32* (*Slc32a1*, #319198), *iCre* (#423321), *Avp* (#401391), *Gfp* (#409018), *Esr1* (#49622). Images were taken using the Zeiss LSM 710 confocal microscope (Zeiss). Cell counts were performed manually with Photoshop software.

Pharmacological treatments

Intra-amygdala AVP injections. Prior to marble burying, adult WT and *Avpr1a*$^{-/-}$ females were bilaterally injected with 1 ng of AVP or 0.9% saline via in-dwelling cannulas using a Hamilton syringe (Hamilton 7635-01) connected to an injector (Model C317IS, Plastics One).

Peripheral antagonist injections. Injections of SRX246 (AVPR1A antagonist, made in-house by the Organic Chemistry Collaborative Core at Columbia University Irving Medical Center, 2 mg/kg, i.p.), SR49059 (AVPR1A antagonist, Millipore Sigma, 2 mg/kg, i.p.), SSR149415 (AVPR1B antagonist, Tocris, 2 mg/kg, i.p.), β-Mercapto-β,β-cyclopentamethylenepropionyl1,O-Me-Tyr2,Orn8-Oxytocin (Oxytocin receptor antagonist, Millipore Sigma, 2 mg/kg, i.p.), or 1% DMSO (Sigma Aldrich, i.p.) were performed in WT adults.

Water intake measurements

Water intake was monitored continuously using the BioDAQ automated system (Research Diets). Mice were habituated for 3–4 days to the BioDaq and 4–5 days to a 7 pm–7 am access feeding schedule. Injections were performed at 7 pm. Water intake was analyzed with the BioDaq software.

Statistics and reproducibility

All behavioral experiments were scored by a trained observer blind to experimental conditions, or scored using an automated system (Ethovision, Med Associates). Data were then processed and analyzed using GraphPad Prism 8. First, significant outliers were excluded using a Grubbs' test. When appropriate, a Shapiro-Wilk test was performed to assess the normality of the sample distribution. Statistical analyses were then conducted using two-way ANOVAs followed by Tukey or Bonferroni post hoc tests (including repeated measure (RM) ANOVAs for marble burying test), one-way ANOVA followed by Tukey post hoc test, Kruskal-Wallis test followed by Dunn's post hoc test, Mixed-effects analysis followed by Bonferroni post hoc test, and unpaired *t*-tests when appropriate. The significance threshold was held at $\alpha = 0.05$, two-tailed (not significant, ns, $p > 0.05$; *$p < 0.05$; **$p < 0.01$; ***$p < 0.001$; ****$p < 0.0001$).

Reporting summary

Further information on research design is available in the Nature Portfolio Reporting Summary linked to this article.

Data availability

All data generated in this study are provided in the Source Data file. Source data are provided with this paper.

Code availability

Code for an automated pipeline generated in ImageJ used to estimate the density of boutons in each region is available at https://github.com/seh2232/ImageJ_Nuclei_Bouton_Counter_Batch) https://doi.org/10.5281/zenodo.17094531[48].

References

1. Stroud, L. R., Salovey, P. & Epel, E. S. Sex differences in stress responses: social rejection versus achievement stress. *Biol. Psychiatry* **52**, 318–327 (2002).
2. Benenson, J. F. et al. Social exclusion: more important to human females than males. *PloS One* **8**, e55851 (2013).
3. Clauss, N. & Byrd-Craven, J. Exposure to a sex-specific stressor mitigates sex differences in stress-induced eating. *Physiol. Behav.* **202**, 26–35 (2019).
4. Collaborators, C.-M. D. Global prevalence and burden of depressive and anxiety disorders in 204 countries and territories in 2020 due to the COVID-19 pandemic. *Lancet* **398**, 1700–1712 (2021).
5. Beck, K. D. & Luine, V. N. Sex differences in behavioral and neurochemical profiles after chronic stress: role of housing conditions. *Physiol. Behav.* **75**, 661–673 (2002).
6. Goel, N. & Bale, T. L. Examining the intersection of sex and stress in modelling neuropsychiatric disorders. *J. Neuroendocrinol.* **21**, 415–420 (2009).
7. Tan, T. et al. Neural circuits and activity dynamics underlying sex-specific effects of chronic social isolation stress. *Cell Rep.* **34**, 108874 (2021).
8. Arakawa, H. Ethological approach to social isolation effects in behavioral studies of laboratory rodents. *Behav. Brain Res.* **341**, 98–108 (2018).
9. Walker, D. M., Cunningham, A. M., Gregory, J. K. & Nestler, E. J. Long-Term Behavioral Effects of Post-weaning Social Isolation in Males and Females. *Front Behav. Neurosci.* **13**, 66 (2019).
10. Luciano, D. & Lore, R. Aggression and social experience in domesticated rats. *J. Comp. Physiol. Psychol.* **88**, 917–923 (1975).
11. Yorgason, J. T., Espana, R. A., Konstantopoulos, J. K., Weiner, J. L. & Jones, S. R. Enduring increases in anxiety-like behavior and rapid nucleus accumbens dopamine signaling in socially isolated rats. *Eur. J. Neurosci.* **37**, 1022–1031 (2013).
12. Manning, C. J., Dewsbury, D. A., Wakeland, E. K. & Potts, W. K. Communal nesting and communal nursing in house mice, Mus musculus domesticus. *Anim. Behav.* **50**, 741–751 (1995).
13. Palanza, P. Animal models of anxiety and depression: how are females different?. *Neurosci. Biobehav Rev.* **25**, 219–233 (2001).
14. Francois, M., Canal Delgado, I., Shargorodsky, N., Leu, C. S. & Zeltser, L. Assessing the effects of stress on feeding behaviors in laboratory mice. *eLife* **11**, https://doi.org/10.7554/eLife.70271 (2022).
15. Veenema, A. H., Bredewold, R. & Neumann, I. D. Opposite effects of maternal separation on intermale and maternal aggression in C57BL/6 mice: link to hypothalamic vasopressin and oxytocin immunoreactivity. *Psychoneuroendocrinology* **32**, 437–450 (2007).
16. Murgatroyd, C. et al. Dynamic DNA methylation programs persistent adverse effects of early-life stress. *Nat. Neurosci.* **12**, 1559–1566 (2009).
17. Oliveira, V. E. M., Neumann, I. D. & de Jong, T. R. Post-weaning social isolation exacerbates aggression in both sexes and affects the vasopressin and oxytocin system in a sex-specific manner. *Neuropharmacology* **156**, 107504 (2019).
18. Hernandez, V. S. et al. Hypothalamic Vasopressinergic Projections Innervate Central Amygdala GABAergic Neurons: Implications for Anxiety and Stress Coping. *Front Neural Circuits* **10**, 92 (2016).
19. Tribollet, E., Audigier, S., Dubois-Dauphin, M. & Dreifuss, J. J. Gonadal steroids regulate oxytocin receptors but not vasopressin receptors in the brain of male and female rats. An autoradiographical study. *Brain Res* **511**, 129–140 (1990).
20. Loup, F., Tribollet, E., Dubois-Dauphin, M. & Dreifuss, J. J. Localization of high-affinity binding sites for oxytocin and vasopressin in the

human brain. An autoradiographic study. *Brain Res* **555**, 220–232 (1991).
21. Rosso, M. et al. Reliability of common mouse behavioural tests of anxiety: A systematic review and meta-analysis on the effects of anxiolytics. *Neurosci. Biobehav Rev.* **143**, 104928 (2022).
22. Langer, E., Einat, H. & Stukalin, Y. Similarities and dissimilarities in the effects of benzodiazepines and specific serotonin reuptake inhibitors (SSRIs) in the defensive marble burying test: A systematic review and meta-analysis. *Eur. Neuropsychopharmacol.* **36**, 38–49 (2020).
23. Wang, Z. J. et al. Molecular and cellular mechanisms for differential effects of chronic social isolation stress in males and females. *Mol. Psychiatry* **27**, 3056–3068 (2022).
24. Bale, T. L. & Epperson, C. N. Sex differences and stress across the lifespan. *Nat. Neurosci.* **18**, 1413–1420 (2015).
25. Hodes, G. E. & Epperson, C. N. Sex Differences in Vulnerability and Resilience to Stress Across the Life Span. *Biol. Psychiatry* **86**, 421–432 (2019).
26. Francois, M., Fernandez-Gayol, O. & Zeltser, L. M. A Framework for Developing Translationally Relevant Animal Models of Stress-Induced Changes in Eating Behavior. *Biol. Psychiatry* https://doi.org/10.1016/j.biopsych.2021.06.020 (2021).
27. Fabio, K. et al. Synthesis and evaluation of potent and selective human V1a receptor antagonists as potential ligands for PET or SPECT imaging. *Bioorg. medicinal Chem.* **20**, 1337–1345 (2012).
28. Landgraf, R. & Neumann, I. D. Vasopressin and oxytocin release within the brain: a dynamic concept of multiple and variable modes of neuropeptide communication. *Front Neuroendocrinol.* **25**, 150–176 (2004).
29. Ludwig, M. et al. Regulation of activity-dependent dendritic vasopressin release from rat supraoptic neurones. *J. Physiol.* **564**, 515–522 (2005).
30. Spiteri, T. et al. The role of the estrogen receptor alpha in the medial amygdala and ventromedial nucleus of the hypothalamus in social recognition, anxiety and aggression. *Behav. Brain Res.* **210**, 211–220 (2010).
31. Chen, P. B. et al. Sexually Dimorphic Control of Parenting Behavior by the Medial Amygdala. *Cell* **176**, 1206–1221 e1218 (2019).
32. Ross, M. Affect, facial regard, and reactions to crowding. *J. Pers. Soc. Psychol.* **28**, 69–76 (1973).
33. Brown, K. J. & Grunberg, N. E. Effects of housing on male and female rats: crowding stresses male but calm females. *Physiol. Behav.* **58**, 1085–1089 (1995).
34. Landgraf, R. The involvement of the vasopressin system in stress-related disorders. *CNS Neurol. Disord. Drug Targets* **5**, 167–179 (2006).
35. Hochgerner, H. et al. Neuronal types in the mouse amygdala and their transcriptional response to fear conditioning. *Nat. Neurosci.* **26**, 2237–2249 (2023).
36. Zelikowsky, M. et al. The Neuropeptide Tac2 Controls a Distributed Brain State Induced by Chronic Social Isolation Stress. *Cell* **173**, 1265–1279 e1219 (2018).
37. Weera, M. M. et al. Generation of a CRF(1)-Cre transgenic rat and the role of central amygdala CRF(1) cells in nociception and anxiety-like behavior. *eLife* **11**, https://doi.org/10.7554/eLife.67822 (2022).
38. Wang, Y. et al. Multimodal mapping of cell types and projections in the central nucleus of the amygdala. *eLife* **12**, https://doi.org/10.7554/eLife.84262 (2023).
39. Tye, K. M. et al. Amygdala circuitry mediating reversible and bidirectional control of anxiety. *Nature* **471**, 358–362 (2011).
40. Bourhy, L. et al. Silencing of amygdala circuits during sepsis prevents the development of anxiety-related behaviours. *Brain* **145**, 1391–1409 (2022).
41. Bielsky, I. F., Hu, S. B. & Young, L. J. Sexual dimorphism in the vasopressin system: lack of an altered behavioral phenotype in female V1a receptor knockout mice. *Behav. Brain Res* **164**, 132–136 (2005).
42. De Vries, G. J., al-Shamma, H. A. & Zhou, L. The sexually dimorphic vasopressin innervation of the brain as a model for steroid modulation of neuropeptide transmission. *Ann. N. Y Acad. Sci.* **743**, 95–120 (1994).
43. Sivukhina, E. V. & Jirikowski, G. F. Oxytocin, but not arginine-vasopressin neurons project from the hypothalamus to amygdala in human: DiI-based tracing study in postmortem brain. *J. Chem. Neuroanat.* **111**, 101882 (2021).
44. Barchiesi, R. et al. Stress-induced escalation of alcohol self-administration, anxiety-like behavior, and elevated amygdala Avp expression in a susceptible subpopulation of rats. *Addict. Biol.* **26**, e13009 (2021).
45. Cacioppo, J. T. et al. Loneliness across phylogeny and a call for comparative studies and animal models. *Perspect. Psychol. Sci.* **10**, 202–212 (2015).
46. Santini, Z. I. et al. Social disconnectedness, perceived isolation, and symptoms of depression and anxiety among older Americans (NSHAP): a longitudinal mediation analysis. *Lancet Public Health* **5**, e62–e70 (2020).
47. Taylor, S., Abramowitz, J. S. & McKay, D. Non-adherence and non-response in the treatment of anxiety disorders. *J. anxiety Disord.* **26**, 583–589 (2012).
48. François, M. et al. Amygdala AVPR1A mediates susceptibility to chronic social isolation in female mice. Github, https://doi.org/10.5281/zenodo.170945312023
49. Ho, S. Created in BioRender. https://BioRender.com/yt6yv9t (2025).

Acknowledgements

We would like to thank Dr. Mu Yang for help with behavioral experiments, Dominique Bozec, Jay Davis, Nikolay Shargorodsky, Lianqun Yang and Rebecca Cooper for technical assistance, Dr. Dave Olson for generating the *Avpr1a*-Cre line, Shuliang Deng and Dr. Vidhu Thaker for transcriptomic analyses that were not included, Dr. Amit Zeisel for sharing dataset before publication, and Dr. Gerard Karsenty for helpful discussions. This work was funded by the NIH R01MH113353 (L.M.Z.), R01MH117127 (G.D.), and R01HD098184 (G.D.), the Klarman Family Foundation (L.M.Z.), and the Russell Berrie Foundation (L.M.Z.). This research was supported by several core facilities at Columbia University: NCI Cancer Center Support Grant P30CA013696 for the Confocal and Specialized Microscopy and Molecular Pathology shared resources of the Herbert Irving Comprehensive Cancer Center; NIDDK Diabetes Research Center Support Grant P30DK063608 for the Advanced Tissue Pathology and Imaging Core, Institute of Genomic Medicine NeuroBehavior Core; and Organic Chemistry Collaborative Center. NIDDK Diabetes Research Center Support Grant P30DK020572 (MDRC) for the Molecular Genetics Core at the University of Michigan.

Author contributions

M.F. and L.M.Z. designed the experiments and wrote the manuscript. M.F. performed and coordinated the experiments. K.L.V. and I.C.D. performed behavioral testing and quantified anterograde tracing. L.A.C.S. performed control viral injections and histology. A.L., M.K., T.D., B.W., and K.G.B. performed behavioral testing. N.R.L. performed imaging and generated figures, and edited the manuscript. R.H. performed the initial experiments implicating *Avpr1a*. D.N. analyzed the Zeisel data set and performed some statistical analyses. S.E.H. developed the analytical pipeline for bouton quantification. Y.O. and C.D.M. performed electrophysiological recordings. E.M.L. and G.D. generated the *Avp*-Flp and *Avpr1a*^{flox} mouse lines.

Competing interests

Columbia University has filed a patent application related to this work for which L.M.Z. and M.L.P.J.F. are inventors. The pending US patent application no. is US 18/814,287. The remaining authors declare no competing interests.

Additional information

Supplementary information The online version contains supplementary material available at https://doi.org/10.1038/s41467-025-64742-y.

Correspondence and requests for materials should be addressed to Lori M. Zeltser.

Peer review information *Nature Communications* thanks the anonymous reviewer(s) for their contribution to the peer review of this work. A peer review file is available.